# Methodology for consideration of different load cases in the design of a sensor-integrating, gentelligent antenna

**Proceedings of the Design Society, Volume 5: ICED25**
https://doi.org/10.1017/pds.2025.10254

# Methodology for consideration of different load cases in the design of a sensor-integrating, gentelligent antenna

**Alessio Galfione[1,✉], Sören Meyer zu Westerhausen[2], Timo Stauß[2], Max Leo Wawer[2], Salvatore Ameduri[3], Giovanni Totaro[3], Marco Esposito[1], Roland Lachmayer[2] and Marco Gherlone[1]**

*[1] Politecnico di Torino, Italy, [2] Leibniz University Hannover, Germany, [3] CIRA Italian Aerospace Research Centre, Italia*

✉ alessio.galfione@polito.it

**ABSTRACT:** Sensor-integrating, gentelligent components "inherit" data on operational loads from one generation to the next for design optimisations and require an optimal sensor placement (OSP) to make accurate decisions based on this data. The OSP can be very time-consuming, and most studies focus only on one load case. To address this issue, a methodology for OSP for several load cases, based on the region-growing algorithm for FEM simulation data (RGA4FEM) for solution space reduction, is presented. For validation of the methodology's applicability, a case study is carried out for a boom of a satellite antenna. The results show that region-based approaches are slower to converge but need smaller populations to find global optima with a genetic algorithm. Furthermore, high robustness is achieved for the most demanding parameters on all load cases in a single optimisation.

**KEYWORDS:** mechatronics, design process, case study, optimal sensor placement, modal method

## 1. Introduction

In recent years, smart products integrating electronic components into load-carrying structures have been growing in popularity (Brenneis et al., 2014; Zheng et al., 2019; Kirchner et al., 2024). This trend is observed in the aerospace field alongside an increasing interest in structural health monitoring and digital twins thanks to structure-integrated and embedded sensors and sensor networks (Li et al., 2022; Meyer zu Westerhausen et al., 2024a; Koesters et al., 2024). These acquired data are relevant for monitoring and real-time decision-making. For example, they can improve condition- and damage-based maintenance but are also of high value for designing next-generation products and structural components. Information on operational loads can be used for the adaption of the following component generation to such loads in the context of product generation development (Albers et al., 2018). If the sensors are embedded directly into the component, e. g., in a composite material's layers, this information becomes an integral part of the product. Therefore, it is "inherited" from one generation to the next in the paradigm of technical inheritance. From these specific characteristics, the term "gentelligent" is defined for such structural components (Lachmayer et al., 2014; Lachmayer and Mozgova, 2021).
Therefore, reliable data acquisition and compliance with data quality dimension (correctness, completeness, integrity, etc.) of measured or reconstructed operational loads is crucial. Choosing the best-suited positions for measurement systems, such as strain gauges, is essential to achieve these goals. For this reason, an Optimal Sensor Placement (OSP) is necessary to find a sensor layout with a minimal measurement error (Meyer zu Westerhausen et al., 2024b). However, such optimisation algorithms struggle to find global optima when the solution space is large, returning suboptimal solutions. Furthermore, an optimal sensor placement for one specific load case might not be optimal for a different

loading scenario (Saleem and Jo, 2021). Therefore, there is a need for a methodology that allows optimal sensor placement for different load cases while reducing the solution space for more robust and computationally efficient optimisations. Since such methods are not emphasised enough in the literature, this paper addresses this issue in the following. As a result, the structure is organised in the following way. In Section 2, an overview of related works is given. In this context, a brief introduction to shape and load sensing techniques for deformation and load reconstruction is provided, along with relevant studies on related issues in OSP. Building upon the identified research gap, a methodology for a more robust and efficient OSP for multiple load cases is presented in Section 3. A numerical case study is conducted in Section 4 to demonstrate the proposed methodology's applicability. The method is applied to an antenna for space applications. Finally, Section 5 concludes this paper and gives an outlook on future works.

## 2. Related works

Deformations and loads occurring during the product use phase can be reconstructed using shape and load sensing techniques from strain measurements at discrete positions. These techniques can be sorted into four different groups following (Gherlone et al., 2018): (1) methods employing Artificial Neural Networks (ANN); (2) methods based on a finite-element discrete variational principle; (3) methods based on the numerical integration of experimental strains; and (4) methods using global or piecewise continuous basis functions to approximate the displacement field.

In the first group, an increasing trend of publications is observed with a specific interest in the field of artificial intelligence for engineering design, e.g. to predict loads from measured strains (Khaleel et al., 2023; Xu et al., 2023). However, these ANN applications show high dependence on the training data and are challenging to implement. The complexity comes from the need for a good understanding of the several kinds of neural networks, of the different activation functions, and of many other parameters (Tripathi et al., 2021). In the second group, (Tessler and Spangler, 2005) published the inverse Finite Element Method (iFEM), the most well-known shape-sensing technique (Gherlone et al., 2018). This method has proven to be very accurate and flexibly applicable due to the independence of material characteristics. However, it needs a considerable quantity of sensors. Moreover, it is challenging to implement because of specific element formulations, which are not available in commercial tools or open-source codes (Esposito and Gherlone, 2020; Esposito, 2024). In the third group, Ko's displacement theory gained much interest for its simple implementation and the need for only a few sensors. This technique integrates strain measurements into displacement and slope equations derived from the Euler-Bernoulli beam theory (Ko et al., 2007; Gherlone et al., 2018). A disadvantage of this method is the applicability only to structures that can be approximated by a beam (Esposito and Gherlone, 2020). The most often mentioned shape-sensing technique in the fourth group is the Modal Method (MM), which was initially introduced by (Foss and Haugse, 1995). This technique assumes the vector of displacements of a structure, $\boldsymbol{u}$, to be the linear combination of the natural mode shapes with specific coefficients. Using the same coefficients, a similar assumption is made for the vector of strains, $\boldsymbol{\varepsilon}$, defined as a linear combination of the modal strains. The modal shapes and strains are saved in the modal shape matrices, $\boldsymbol{\phi}_d$ and $\boldsymbol{\phi}_s$, respectively. The relationship between the measured strains and the reconstructed displacements is presented in Equation (1).

$$u = \phi_d(\phi_s^T\phi_s)^{-1}\phi_s^T\varepsilon \tag{1}$$

Therefore, prior knowledge of the structure's mode shapes is required, which could be derived from experiments or finite element (FE) simulations. However, the numerical process requires the number of strain sensors to exceed the number of modes included. Therefore, choosing the mode shapes most relevant to the reconstruction of the part deformation is essential. As a result of its intrinsic knowledge of the structure, in literature, the MM was found to be very accurate with only a few sensors (Esposito and Gherlone, 2020). Because of its advantages in comparison to ANNs, iFEM, and Ko's displacement theory, the MM has been chosen for further consideration.

The MM has proven to be very accurate. However, an OSP is still necessary to minimise the number of sensors and reduce error in reconstructing the deformed shape or, alternatively, to maximise accuracy for a given number of sensors. Various optimisation algorithms are used in the literature on OSP for structural health monitoring, a broader research field in which shape sensing is commonly included. Examples are genetic algorithms, particle swarm optimisation, monkey algorithms, firefly algorithms, ant colony optimisation, and other algorithms (Tan and Zhang, 2020). Since, in most applications, the OSP in shape sensing aims to minimise the error of the displacement reconstruction in the three

directions, multi-objective optimisation is commonly used. Due to its characteristic robustness in finding global optima, the NSGA-II is often used in this context. Several other studies in the literature apply the MM for shape sensing. Many of these studies also perform an OSP to apply the MM effectively.
Gherlone et al. 2018 also applied the modal method to a wing-shaped plate, selecting six modes for the analysis. Based on the simulation results, the authors also conducted an experimental study using 44 linear strain gauges on two parallel lines. However, no OSP was performed in this study, and only a single load case was considered in the experiments (Gherlone et al., 2018). Another study was conducted by (Esposito and Gherlone, 2020) on a composite aircraft wing box. In this study, an OSP was carried out to apply the MM using a single-objective genetic algorithm. Here, the deformed shape reconstruction was carried out on a single numerical load case, the bending of the wing box. In the study of (Valoriani et al., 2022), the MM was applied to the example of an unmanned aerial vehicle wing and compared with Ko's displacement theory. As in the studies mentioned above, the MM yielded results with very low errors, but there was neither any OSP performed nor different load cases considered. Another approach for the application of the MM was presented by (Esposito, 2024), where the MM was coupled with the iFEM. The work aimed to overcome the issue of the large number of sensors required for iFEM by pre-expanding the strain field. This new approach was applied to the example of a stiffened plate in a numerical and an experimental study. However, this study did not include several load cases either. The work of (Meng et al., 2022) differs from the studies above as it incorporates various load cases and loading scenarios in the shape sensing of a round tube and a composite wing model. An enhanced form of the MM was applied for these two examples, and the results were very accurate. However, even though different load cases were considered, the sensor positions were chosen without an OSP, a process which could improve the results. In the work of (Sun and Büyüköztürk, 2015), the focus is set differently from that of the studies mentioned earlier. In this case, addressing the monitoring of a civil structure, the detection of specific modes in the use phase is investigated instead of the deformed shape reconstruction with the MM. Therefore, the OSP is performed for different resulting modes as the load cases of the structures under consideration using the so-called modal assurance criterion (MAC) for evaluation. The OSP is performed as multi-objective optimisation under constraints for the MAC in the objective functions for ten included modes as load-cases to detect. An experimental study was conducted for the derived OSP, and the identification of the modes was accurate.
From all the studies presented above, it becomes clear that the MM is well-suited for various applications. However, the OSP is always performed for only one load case in each study or, as in the case of (Sun and Büyüköztürk, 2015), it is not carried out for shape sensing with the MM. In real-world applications, multiple load cases occur on a structure during its use phase. Not considering this fact can lead to inaccuracies when an unexpected load case occurs. A possible approach to overcome this issue could be to evaluate the similarity of sensor positions, resulting in optimal solutions for different load cases. This solution is proposed by (Meyer zu Westerhausen et al., 2024a) for the OSP for manufacturing and product use. A problem with this approach might occur when the load cases considered are too many and too different, resulting in very different OSPs per load case. To overcome this issue, a different approach is presented in the following.

## 3. Proposed methodology for OSP for different load cases

From the studies presented in Sections 1 and 2, there are two major problems of an OSP for different load cases. They are the requirements for high accuracy for all of them and the large solution space, resulting in many placement options. Consequently, excessive iterations may be necessary to achieve convergence for all load cases, and a global optimum might not be obtained. A new methodology is proposed for OSP for multiple load cases to reduce the risk of finding only local optima. This method focuses on narrowing the solution space, which, in turn, improves the computational speed. A general procedure to apply this methodology is shown in Figure 1.
Initially, finite elements (FE) simulations must be conducted for all the load cases to be considered in the design of the part and the OSP. Afterwards, the strain component that is most representative in all the load cases must be selected. For instance, in the case of an OSP for load cases where the longitudinal strains are most relevant, this component is chosen. Examples can be a cantilever beam subject to bending or to a force in the longitudinal direction. The selected component of strain and all displacement components are exported for each element in the FE model for all load cases. Furthermore, the strains for the selected strain component and all displacement components are exported for the eigenmodes of the part under consideration derived from the simulations. The displacements and strains modal shape

matrices $\boldsymbol{\phi}_d$ and $\boldsymbol{\phi}_s$, respectively, are built from these exported data. To select the most relevant modes for shape sensing with the MM, the criterion presented in (Bogert et al., 2003) must be applied.

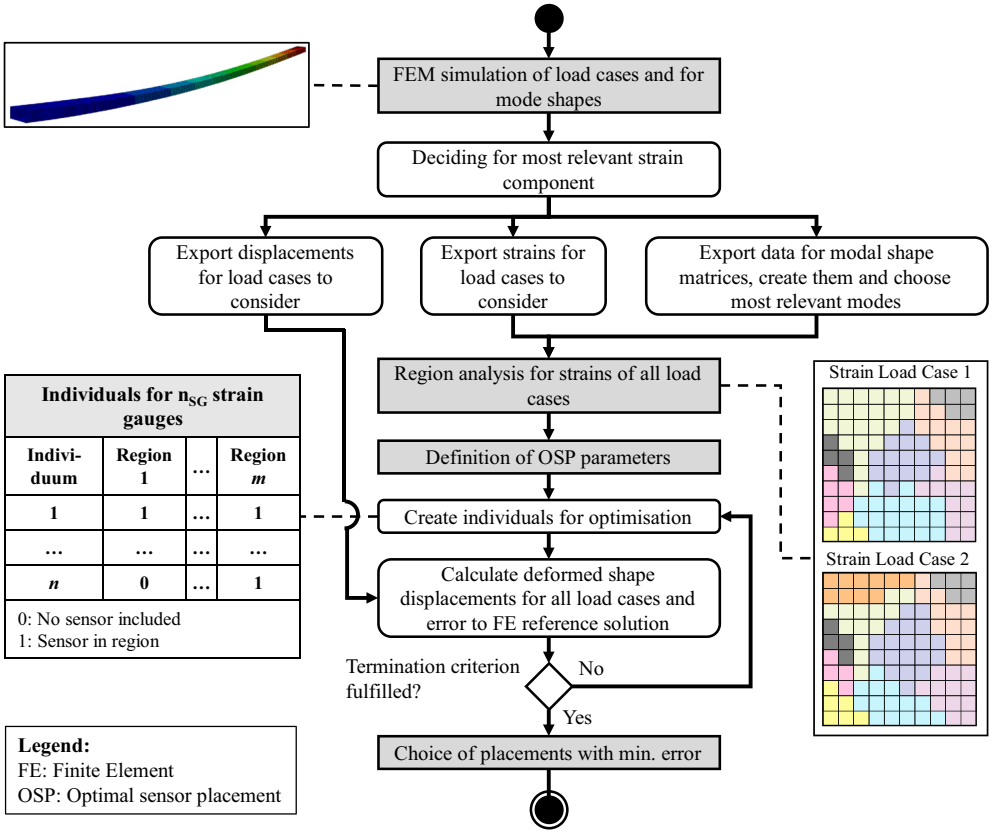


**Figure 1. Procedure of the proposed methodology for OSP with narrowed solution space for several load cases**

A so-called region analysis is performed after all the data for calculations and for OSP are exported. This step in the procedure is based on the "Region Growing Algorithm for Finite Element Modelling (RGA4FEM)" published algorithm, described in detail in (Meyer zu Westerhausen et al., 2024b). In this algorithm, elements of an FE model are clustered into regions if their strain values are not distinguishable by a strain sensor due to the measurement sensitivity. Furthermore, elements below the minimal detectable strain, $\varepsilon_{min}$, are excluded from further consideration. The value of $\varepsilon_{min}$ can be defined, for example, by the noise level of the sensing system. The RGA4FEM is adapted from its initial purpose in the reliability analysis of sensor networks to reduce the solution space for OSP. The adapted approach for the proposed methodology finds regions for each load case in the first step and then searches for overlapping regions in the second step. These intersections of similar regions are then combined for all considered load cases, as described for different strain components by (Meyer zu Westerhausen et al., 2024b). This combination of elements into regions is based on the load cases strains and reduces the solution space. Sensors cannot be placed in all elements but only at the region centroids since the position of a sensor inside a region is irrelevant. As a result of the region analysis, the region centroid coordinates and the strains at these positions are exported for the OSP.

Then, the OSP is performed using the NSGA-II as a genetic algorithm for multi-objective optimisation since it is known for being robust in finding global optima (Deb et al., 2002; Meyer zu Westerhausen et al., 2024a).

Before this step in the procedure can be carried out, the parameters for the OSP must be selected. These parameters include the maximum number of generations and the population size. Moreover, the deformed shape reconstruction error must be defined as the objective function. A corresponding tolerance for such error must be determined to abort the optimisation if a solution is found. This definition of a goal to reach for accuracy should increase the computational speed because the optimisation does not look for the best solution but for one that is "good enough". Therefore, in each generation, for each individual, the deformed shape is reconstructed using the modal method based on the strain

measurements for all considered load cases. Then, the deviation from the FE reference solution is calculated for each load case. The process is repeated until one of the following three criteria is fulfilled.

1) The above-mentioned error value is lower than the tolerance for all load cases.
2) The predefined maximal number of iterations is exceeded.
3) The change in the spread of the Pareto front is smaller than a certain tolerance.

At the end of the optimisation, the most suitable sensor placement solution is selected as the OSP for the shape-sensing task for the considered load cases.

## 4. Numerical case study for a gentelligent antenna

The methodology described above is applied and evaluated on a numerical case study of a gentelligent space structure. This structure is a boom for large deployable reflectors (LR-BOOM), described in detail in (Giusto et al., 2021) and (Nicola et al., 2023) and which is shown in Figure 2 a). It is designed to integrate a sensing system for shape sensing to get insights into operational loads for further development in the following product generation and for structural health monitoring. The structure is built of carbon fibre reinforced polymer (CFRP) in a tubular grid architecture, realised by an automated winding technique, which allows the structural integration of sensors. For this sensor integration, 16 single linear strain gauges will be used. The FE model of the structure is shown in Figure 2 b). It is used in the simulations carried out in the commercial software MSC Patran using the MSC Nastran solver. Due to the grid-like architecture of the LR-BOOM, one-dimensional CBAR elements are used. A region of 40 *mm* is clamped on one side. On the other end, a region 40 *mm* wide, where the loads are applied, is modelled with two-dimensional CQUAD4 elements. However, for the OSP, only the 13'720 beam elements that are free to deform are considered.

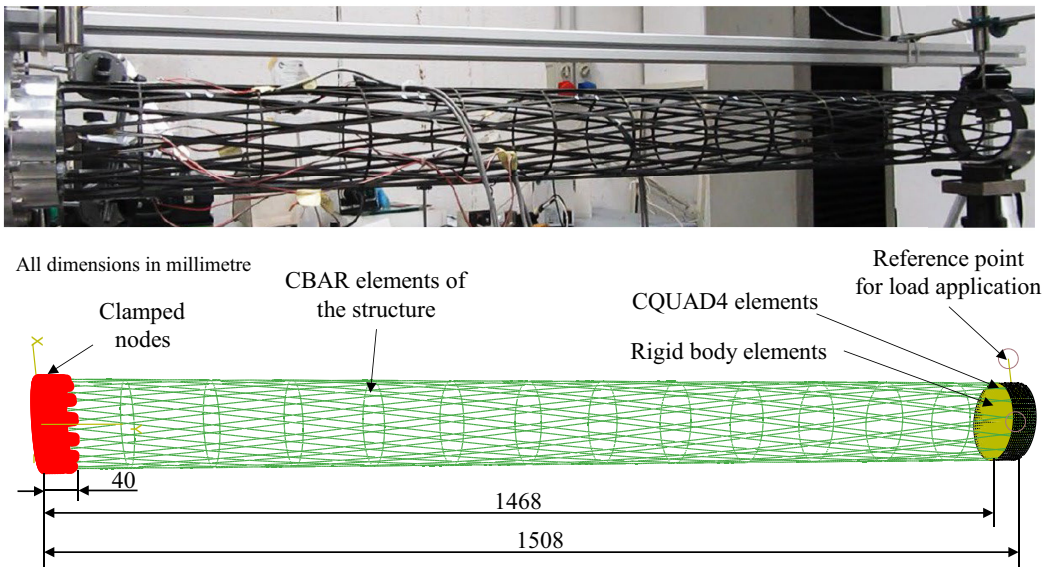


**Figure 2. LR-BOOM in the real-life design (a) and the FE model built up for the OSP (b)**

For the design of the gentelligent LR-BOOM, the three load cases depicted in Figure 3 are considered. The LR-BOOM is assumed to be a cantilever beam for all three load cases. The clamped end on the left side models the clamping to the satellite's main body. The loads are applied to a single reference node, placed at the centre of the section, and transmitted to the nodes facing the reflector through rigid body elements in the FE model. This load application region models the connection of the boom to the reflector. Only the local longitudinal strains are available since beam elements are selected to model the structure. To reconstruct the deformed shape of the structure, the relevant modes were chosen as described in Section 3 using the method of (Bogert et al., 2003). The number of sensors available is fixed and equal to 16. This number comes from a specific experimental setup in which the data acquisition system can read a maximum of 16 strain gauges. For applying 16 strain gauges, a maximum of 15 modes could be selected, as described in Section 2. However, only modes 1, 2, 3, 5, 10, 12, 29, and 187 were chosen from an ABC analysis of the first 200 modes' strain energy contributions. The remaining modes

were excluded from the study because their strain energy contributions were minimal, and they were degrading the results.
For further processing in the proposed methodology, the strain data are exported from MSC Patran to a *.txt file for all beam elements and each load case. The strains and displacements for each chosen mode are also exported from MSC Patran to a *.txt file.

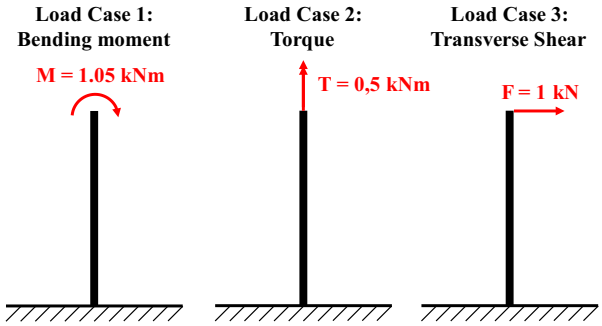


**Figure 3. Load cases and loads applied to the LR-BOOM in the case study**

The data exported in the *.txt files are used for the region analysis with the RGA4FEM, as described in Section 3. For this application, the minimal detectable strain is set to $\varepsilon_{min} = 0.1\ \mu m/m$. This parameter was derived for measurements performed using HBM 1-LY11-6/120 strain gauges and an HBM QuantumX840B data acquisition system on a beam-like structure under bending load. Measurements were performed for the unloaded structure and different loads, where each measurement took 90 s. From the recorded strain measurements of the strain gauges, the noise level and the standard deviation of measurements were derived, leading to the above-mentioned value of $\varepsilon_{min}$. To build the regions, the strains of the elements considered for each iteration of region growth are compared to the average strain of the region. If the difference is within a tolerance of $t_{reg} = 0.01$ % the element becomes part of that region. This tolerance value was selected to avoid including elements with significantly different strains in a region, which could lead to inaccuracies. Through this process, 7176 regions are identified from the intersections of the results for all three load cases. Therefore, the quantity of placement options is reduced to 52.3% of the case with all elements as placement options.
For the OSP, three different approaches are considered in the following to demonstrate the applicability of the proposed methodology:

1. Element-based OSP (ElemOSP):
   All elements are considered placement options for all load cases, and only the strains of the sensor-equipped elements are used for shape sensing. This conventional approach is regarded as a benchmark for the proposed methodology.
2. Region-based OSP (RegOSP):
   All region centroids are considered as placement options for all load cases. Only the measured strains at the centroids of sensor-equipped regions are used for shape sensing.
3. Expanded region-based OSP (ExpRegOSP):
   All region centroids are considered as placement options for all load cases. The measured strains at the centroids of sensor-equipped regions are expanded to all the region's elements. All these values are then used for shape sensing.

The OSP is performed in all approaches using MATLAB's *gamultiobj()* function, which implements a multiobjective genetic algorithm (see (The MathWorks, Inc., 2024a)). The built-in parallel computing option of the function is used on a workstation with an Intel® Core™ i7-5820K CPU @ 3.30 GHz six cores, 12 logical processors, and 16 GB RAM. Two error values per load case are used to evaluate the fitness of each individual of a generation. First, the normalised root mean square error (NRMSE) is calculated as per Equation (2) for the displacement field reconstruction of the whole model. The second evaluation quantity is the maximum relative error at the LR-BOOM tip (TipErr), computed using

Equation (3).

$$NRMSE = \frac{\sqrt{\frac{\sum_i \sum_j (d_{i,j}^{FEM} - d_{i,j}^{MM})^2}{3n}}}{MaxDisp} \tag{2}$$

$$TipErr = \max_{i,j} \frac{|d_{i,j}^{FEM} - d_{i,j}^{MM}|}{MaxDisp} \tag{3}$$

In these equations, $d$ is the displacement. The superscripts *FEM* and *MM* characterise the displacements as coming from the FEM analysis or the MM reconstruction, respectively. The index $i = x,y,z$ represents the direction of the displacement. The index $j$ represents the node for which the displacement is computed, $n$ is the number of nodes in the model. In the *NRMSE* definition, $j$=1,2,...,$n$, while in the *TipErr* definition $j$ only includes the nodes positioned next to the loaded part of the model. The ones that are also nodes of the shell elements. Finally, the normalising quantity is $MaxDisp = \max_{i,j} d_{i,j}^{FEM}$, the maximum displacement of the structure. The three *TipErrs*, one per load case, are used in the optimisation algorithm as objective functions. The optimisation is considered converged to an acceptable sensor configuration if all *TipErrs* are lower than the $t_{tip}$ tolerance. On the other hand, the three *NRMSEs* are used as constraints to the problem. If, for a sensor configuration, at least one of the *NRMSEs* is higher than the $t_{NRMSE}$ tolerance, this configuration is not accepted as a possible solution, and its fitness function (*TipErrs*) is penalised. In the end, there will be three objective functions (*TipErrs* and three constraints (*NRMSEs*). This approach ensures that the selected sensor configuration provides acceptable global results and accurate local results in the area of interest, the free end. As mentioned above, each configuration can use 16 strain sensors.

Two studies have tested the proposed algorithm to demonstrate its applicability. In the first study, the tolerance of the *NRMSEs* ($t_{NRMSE}$) is set to 0.05 and in the second to 0.10. These values were chosen to set tolerances that were not too strict on the global deformed shape reconstruction, so convergence is still possible in the optimisation. Moreover, preliminary tests showed that this tolerance barely affects the convergence speed in an OSP. To analyse the influence of the tolerance on the *TipErr* ($t_{tip}$) and of the population size (*PS*) on the computational speed, the following values of these quantities are tested. For both studies, $t_{tip}$ is tested with six values: 0.02, 0.03, 0.04, 0.06, 0.08 and 0.1. Furthermore, three *PS*s are tested, using 100, 200, and 500 individuals per generation. Besides, in all conducted OSPs, the initial population is generated as a latin hypercube sample using the *lhsdesign()* MATLAB function (see (The MathWorks, Inc., 2024b)). Then, a check is performed to ensure that no individual has repeated sensors and to correct the ones that do with random sensors. Furthermore, each optimisation setup is tested 20 times to average the convergence time, which strongly relies on the starting population.

In Figure 4, the results of the studies that were conducted are shown. In these plots, some points are marked with a red circle. These points are OSP setups, where it converged for less than 25% of the tries, which shows that the convergence to an optimum is less reliable. For both values of $t_{NRMSE}$ this risk occurs in cases where a small value for $t_{tip}$ is chosen. Moreover, the risk increases for smaller values of *PS*, since there is a smaller chance of finding optimal solutions than with larger populations.

For all combinations of *PS*, $t_{NRMSE}$ and $t_{tip}$, the convergence to an optimal solution is reached faster if the $t_{tip}$ values are larger since it is easier to satisfy the objective functions. Furthermore, regarding computational cost, the expanded region-based approach is comparable to the element-based approach, although the second is slightly faster. On the other hand, the region-based approach is consistently outperformed by the other two methods in terms of computational cost. Besides, the region-based approach showed a higher risk of not converging to an optimal solution even with higher computational time. This result is highlighted by the number of points marked with a red circle or missing for this approach. In contrast, the expanded region-based approach showed more robust solutions when small values for $t_{tip}$ are chosen. The results for this approach are barely marked with a red circle and are available even for small tolerance values, where the other approaches could no longer converge. Quite remarkable is the ability of the expanded region-based approach to find a solution for $t_{tip}$ = 0,02 when $t_{NRMSE}$ = 0.05, the most restrictive set of requirements tested.

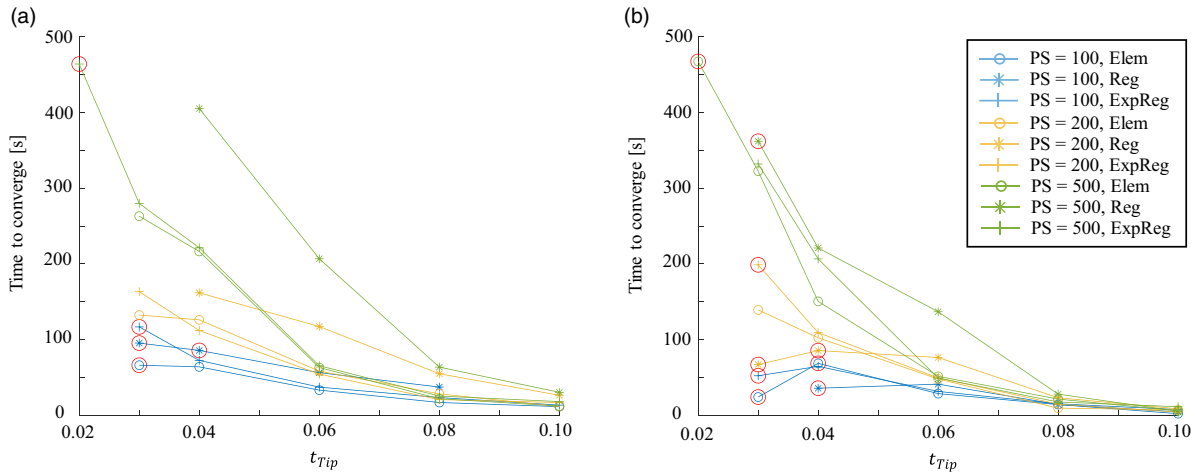


**Figure 4. Comparison of the convergence speed for different population sizes (*PS*) and tolerance for the tip relative error ($t_{tip}$) for a tolerance of the normalised root mean square error of $t_{NRMSE}$ = 0.05 (a) and $t_{NRMSE}$ = 0.01 (b)**

From this comparison, the proposed methodology appears well-suited to perform an OSP for different load cases for shape sensing with the MM. The expanded region-based approach outperforms the conventional element-based approach in terms of robustness for small tolerances. Therefore, this case study demonstrated the applicability of the methods, even though the region-based approach without expansion underperforms the benchmark.

## 5. Conclusion and future work

Integrating sensors into structural components allows data acquisition on operational loads during the product use phase. Due to this acquired data and the derived information being an integral part of the components, they are referred to as gentelligent. The information inherited from one generation to the next allows optimisations in developing the next component generation. To enable reliable data acquisition with correctly derived loading information, an OSP is necessary. This process might be complex when more than one load case and an extensive solution space must be considered.

A methodology with a more robust OSP and, consequently, more efficient optimisation is proposed to reduce the risk of running into local optima or of not finding feasible solutions from the optimisation at all. This approach is based on the use of the so-called RGA4FEM algorithm. This algorithm clusters elements from an FE model into regions based on their strain values and the expected sensitivity of the measurement system. To consider more than one load case, only one strain direction is considered for measurements. The values from all load cases are considered to derive “common” regions as intersections of the ones computed for each load case. As a result, a narrowed solution space is derived since not all elements have to be considered as placement options, only the regions. Furthermore, this technique allows the expansion of the strain measurement from a region sensor to all region elements. This approach includes more information in the shape sensing without reducing the accuracy since the strains are comparable at all locations in a region. In principle, the frequency of the real-time reconstruction is not constrained by the method but by the computational power and sensors’ capabilities.

In a numerical case study, this methodology is applied to the example of a gentelligent antenna in an aerospace application. Three different load cases are considered for the OSP using the NSGA-II as an optimisation algorithm. The objective is to know the displacement of the boom tip on which the reflector is mounted. A comparison is presented between the conventional element-based optimisation approach and two different ones. The first alternative approach considers only the region centroids as solution space (region-based approach). The second one is a region-based approach with measurement expansion to all included elements of a region. In comparison, none of the region-based approaches is more computationally efficient in terms of convergence speed than the element-based approach. However, it was found that in the region-based approaches fewer individuals per generation are necessary to find global optima. This leads to a higher computational efficiency since fewer placement alternatives have to be processed, so optimisations can run significantly faster. Furthermore, the results show that the expanded region-based approach is more robust than the element-based for small tolerances. Moreover,

even though the results presented here are produced on a single load case at a time, a combination of load cases would be accurately reconstructed since it would be a linear combination of linear combinations. The presented results will be analysed in future works in further examples and case studies. Besides, the expanded region-based approach will be tested for shape and load reconstruction when regions are built for a different load amplitude than the one considered for OSP. Different load amplitudes might lead to further varying strains and, therefore, different regions, adding complexity to the problem. Furthermore, implementing the techniques and algorithms in different tools and programming languages requires more effort to apply the methodology. Therefore, combining the steps in a single tool will be addressed to reduce the need to write data into files for export and import. By doing so, computational efficiency could be further increased, and the risk of compatibility errors reduced. Furthermore, future works will address the issue of reliability of the sensor network for monitoring as well. The optimisation will be considering the placement of additional, redundantly measuring sensors besides the needed ones based on the failure probability in dependence of occurring strain amplitudes. For this purpose, the RGA4FEM can be utilised as well, as described in its initial publication in (Meyer zu Westerhausen et al., 2024b). Last, this current version only considered the placement of single linear strain gauges. In future works, an enhancement to the application of fibre optic sensors (FOS) could also be of interest. Such FOS can provide more measurements with fewer sensors, significantly improving the shape-sensing process.

## Acknowledgements

This publication is part of the project PNRR-NGEU which has received funding from the MUR - DM 117/2023. CIRA and POLITO authors would also acknowledge the Italian National Project LR-BOOM for the activities relevant to the boom test article.

## References

Albers, A., Rapp, S., Heitger, N., Wattenberg, F. and Bursac, N. (2018), "Reference Products in PGE – Product Generation Engineering: Analyzing Challenges Based on the System Hierarchy", *Procedia CIRP*, Vol. 70, pp. 469–474. 10.1016/j.procir.2018.02.046.

Bogert, P., Haugse, E. and Gehrki, R. (2003), "Structural Shape Identification from Experimental Strains Using a Modal Transformation Technique", in *Structures, Structural Dynamics, and Materials and Co-located Conferences: 44th AIAA/ASME/ASCE/AHS/ASC Structures, Structural Dynamics, and Materials Conference*, Norfolk, Virginia. 10.2514/6.2003-1626.

Brenneis, M., Ibis, M., Duschka, A. and Groche, P. (2014), "Towards Mass Production of Smart Products by Forming Technologies", *Advanced Materials Research*, Vol. 907, pp. 113–125. 10.4028/www.scientific.net/AMR.907.113.

Deb, K., Pratap, A., Agarwal, S. and Meyarivan, T. (2002), "A fast and elitist multiobjective genetic algorithm: NSGA-II", *IEEE Transactions on Evolutionary Computation*,, Vol. 6 No. No. 2, pp. 182–197. 10.1109/4235.996017.

Esposito, M. (2024), "A novel shape sensing approach based on the coupling of Modal Virtual Sensor Expansion and iFEM: Numerical and experimental assessment on composite stiffened structures", *Computers & Structures*, Vol. 305, p. 107520. 10.1016/j.compstruc.2024.107520.

Esposito, M. and Gherlone, M. (2020), "Composite wing box deformed-shape reconstruction based on measured strains: Optimization and comparison of existing approaches", *Aerospace Science and Technology*, Vol. 99, p. 105758. 10.1016/j.ast.2020.105758.

Foss, G. and Haugse, E. (1995), "Using Modal Test Results to Develop Strain to Displacement Transformations", in *Proceedings of the 13th International Modal Analysis Conference*, Nashville, TN, USA.

Gherlone, M., Cerracchio, P. and Mattone, M. (2018), "Shape sensing methods: Review and experimental comparison on a wing-shaped plate", *Progress in Aerospace Sciences*, Vol. 99, pp. 14–26. 10.1016/j.paerosci.2018.04.001.

Giusto, G., Totaro, G., Spena, P., Nicola, F. de, Di Caprio, F., Zallo, A., Grilli, A., Mancini, V., Kiryenko, S., Das, S. and Mespoulet, S. (2021), "Composite grid structure technology for space applications", *Materials Today: Proceedings*, Vol. 34, pp. 332–340. 10.1016/j.matpr.2020.05.754.

Khaleel, M., Ahmed, A.A. and Alsharif, A. (2023), "Artificial Intelligence in Engineering", *Brilliance: Research of Artificial Intelligence*, Vol. 3 No. 1, pp. 32–42. 10.47709/brilliance.v3i1.2170.

Kirchner, E., Wallmersperger, T., Gwosch, T., Menning, J.D.M., Peters, J., Breimann, R., Kraus, B., Welzbacher, P., Küchenhof, J., Krause, D., Knoll, E., Otto, M., Muhammedi, B., Seltmann, S., Hasse, A., Schäfer, G., Lohrengel, A., Thielen, S., Stiemcke, Y., Koch, O., Ewert, A., Rosenlöcher, T., Schlecht, B., Prokopchuk, A., Henke, E.-F.M., Herbst, F., Matthiesen, S., Riehl, D., Keil, F., Hofmann, K., Pape, F., Konopka, D., Poll, G., Steppeler, T., Ottermann, R., Dencker, F., Wurz, M.C., Puchtler, S., Baszenski, T., Winnertz, M., Jacobs, G.,

Lehmann, B. and Stahl, K. (2024), "A Review on Sensor Integrating Machine Elements", *Advanced Sensor Research*, Vol. 3 No. 4. 10.1002/adsr.202300113.
Ko, W.L., Richards, W.L. and van Tran, T. (2007), "Displacement Theories for In-Flight Deformed Shape Predictions of Aerospace Structures", *NASA/TP-2007-214612*.
Koesters, A., Koetz, F., Bock, M., Fett, M., Breimann, R. and Kirchner, E. (2024), "Methodical Development of a Digital Twin for an Industry Valve", *Machines*, Vol. 12 No. 10, p. 674. 10.3390/machines12100674.
Lachmayer, R. and Mozgova, I. (2021), "Technical Inheritance as an Approach to Data-Driven Product Development", in Krause, D. and Heyden, E. (Eds.), *Design Methodology for Future Products: Data Driven, Agile and Flexible*, Springer eBook Collection, Springer, Cham, pp. 47–64. 10.1007/978-3-030-78368-6_3.
Lachmayer, R., Mozgova, I., Reimche, W., Colditz, F., Mroz, G. and Gottwald, P. (2014), "Technical Inheritance: A Concept to Adapt the Evolution of Nature to Product Engineering", *Procedia Technology*, Vol. 15, pp. 178–187. 10.1016/j.protcy.2014.09.070.
Li, L., Aslam, S., Wileman, A. and Perinpanayagam, S. (2022), "Digital Twin in Aerospace Industry: A Gentle Introduction", *IEEE Access*, Vol. 10, pp. 9543–9562. 10.1109/ACCESS.2021.3136458.
Meng, Y., Xie, C., An, C., Xu, Q. and Yang, C. (2022), "Three-dimensional large deformation reconstruction for slender wing-like structures from strain measurements", *Measurement*, Vol. 204, p. 111969. 10.1016/j.measurement.2022.111969.
Meyer zu Westerhausen, S., Kyriazis, A., Hühne, C. and Lachmayer, R. (2024a), "Design methodology for optimal sensor placement for cure monitoring and load detection of sensor-integrated, gentelligent composite parts", *Proceedings of the Design Society*, Vol. 4, pp. 673–682. 10.1017/pds.2024.70.
Meyer zu Westerhausen, S., Raveendran, G., Lauth, T.-H., Meyer, O., Rosemann, D., Wawer, M.L., Stauß, T., Wurst, J. and Lachmayer, R. (2024b), "Reliability Assessment of Wireless Sensor Networks by Strain-Based Region Analysis for Redundancy Estimation in Measurements on the Example of an Aircraft Wing Box", *Sensors (Basel, Switzerland)*, Vol. 24 No. 13. 10.3390/s24134107.
Nicola, F. de, Totaro, G., Giusto, G., Spena, P., Kiryenko, S. and Das, S. (2023), "An efficient and scalable manufacturing method for CFRP lattice structures for satellite central tube and large deployable antenna boom applications", *CEAS Space Journal*, Vol. 15 No. 1, pp. 183–202. 10.1007/s12567-021-00391-3.
Saleem, M.M. and Jo, H. (2021), "Multi-objective sensor placement optimization for structural response estimation under spatially varying dynamic loading of bridges", *Advances in Structural Engineering*, Vol. 24 No. 10, pp. 2255–2266. 10.1177/1369433221993574.
Sun, H. and Büyüköztürk, O. (2015), "Optimal sensor placement in structural health monitoring using discrete optimization", *Smart Materials and Structures*, Vol. 24 No. 12, p. 125034. 10.1088/0964-1726/24/12/125034.
Tan, Y. and Zhang, L. (2020), "Computational methodologies for optimal sensor placement in structural health monitoring: A review", *Structural Health Monitoring*, Vol. 19 No. 4, pp. 1287–1308. 10.1177/1475921719877579.
Tessler, A. and Spangler, J.L. (2005), "A least-squares variational method for full-field reconstruction of elastic deformations in shear-deformable plates and shells", *Computer Methods in Applied Mechanics and Engineering*, Vol. 194 No. 2-5, pp. 327–339. 10.1016/j.cma.2004.03.015.
The MathWorks, Inc. (2024a), "gamultiobj - Find Pareto front of multiple fitness functions using genetic algorithm", available at: https://mathworks.com/help/gads/gamultiobj.html.
The MathWorks, Inc. (2024b), "lhsdesign - Latin hypercube sample", available at: https://mathworks.com/help/stats/lhsdesign.html.
Tripathi, R.P., Tiwari, M., Dhawan, A., Sharma, A. and Jha, S.K. (2021), "A Survey on Efficient Realization of Activation Functions of Artificial Neural Network", in Kumbhar, V.S. (Ed.), *2021 Asian Conference on Innovation in Technology (ASIANCON): Pune, India, Aug 28-29, 2021, 8/27/2021 - 8/29/2021*, PUNE, India, IEEE, Piscataway, NJ, pp. 1–9. 10.1109/ASIANCON51346.2021.9544754.
Valoriani, F., Esposito, M. and Gherlone, M. (2022), "Shape Sensing for an UAV Composite Half-Wing: Numerical Comparison between Modal Method and Ko's Displacement Theory", *Aerospace*, Vol. 9 No. 9, p. 509. 10.3390/aerospace9090509.
Xu, C., Cao, B.T., Yuan, Y. and Meschke, G. (2023), "Transfer learning based physics-informed neural networks for solving inverse problems in engineering structures under different loading scenarios", *Computer Methods in Applied Mechanics and Engineering*, Vol. 405, p. 115852. 10.1016/j.cma.2022.115852.
Zheng, P., Chen, C.-H. and Shang, S. (2019), "Towards an automatic engineering change management in smart product-service systems – A DSM-based learning approach", *Advanced Engineering Informatics*, Vol. 39, pp. 203–213. 10.1016/j.aei.2019.01.002.